Journal of Applied Fluid Mechanics, Vol. 14, No. 4, pp. 1209-1222, 2021.
Available online at www.jafmonline.net, ISSN 1735-3572, EISSN 1735-3645.
https://doi.org/10.47176/jafm.14.04.32037

An Integrated Turbocharger Matching Program for Internal Combustion Engines

S. Mousavi[1], A. Nejat[1†], S. S. Alaviyoun[2] and M. Nejat[3]

[1] *School of Mechanical Engineering, College of Engineering, University of Tehran, Tehran, Iran*
[2] *Mechanical Engineering, K.N. Toosi University of Technology and Design Department of Iran Khodro Powertrain Company, Tehran, Iran*
[3] *Mechanical Engineering, Iran Khodro Powertrain Company, Tehran, Iran*

†*Corresponding Author Email: nejat@ut.ac.ir*

(Received July 20, 2020; accepted December 22, 2020)

ABSTRACT

Following the global environmental concerns, many automobile manufacturers intend to produce smaller engines, aiming to lower emissions and fuel consumption. As compensation for performance reduction, these engines are equipped with turbochargers. One of the challenges is to select the right turbocharger for a specific engine. In this regard, an integrated zero-dimensional turbocharger and engine simulation program is developed, employing a quasi-steady compressible flow method. The program gives the designer the possibility of observing the performance of different compressor-turbine combinations on an internal combustion engine. Engine details such as fuel, cylinder geometry, heat transfer conditions, valve timing, and spark timing are considered within the engine modeling, and the designer can investigate their effects on the overall performance of the system. Compressor and turbine performances are predicted by their previously provided performance maps (steady-state characteristic curves) and special inter- and extrapolation methods. A new algorithm for turbocharger matching is suggested, and its logics, basic convergence loops, and thermodynamic equations have been described in detail. A database containing digitized compressor and turbine maps and details provided by different manufacturers is created and integrated into the program. An existing turbocharged engine has been tested and also simulated by the program. The accuracy of the program results is evaluated by comparing them with experimental results. The maximum error of modeling the engine and the whole simulation is 1.5% and 16%, respectively. Two other compressor-turbine combinations have been evaluated using the program, one of which is suggested as an alternative.

Keywords: Internal combustion engine; Turbocharger matching; Zero-dimensional simulation; Engine performance simulation; Engine downsizing.

NOMENCLATURE

$BSFC$	Brake Specific Fuel Consumption of t the engine	amb	ambient
C_p	specific heat at constant pressure	c	compressor
$\dot{m}$	mass flow rate	corr	corrected
N	speed	e	exhaust gases
P	total pressure	eng	engine
P_d	pressure drop	f	fuel
R	gas constant	IC	intercooler
T	temperature	in	inlet
V	volume	m	mechanical
$\dot{W}$	power	muff	muffler
y	wastegated mass flow rate percentage	ref	reference
γ	heat capacity ratio	shaft	turbocharger Shaft
η	efficiency	t	turbine
ε	heat exchanger effectiveness	tm	turbine-mechanical
a	air	vol	volumetric
AF	air filter		

1. INTRODUCTION

As a consequence of its adverse environmental effects and health issues such as the greenhouse effect and acid rains, the continuously increasing emission level has been globally of great concern in recent years. Therefore, many countries across the world have implemented stringent emission regulations. Many car manufacturers put engine downsizing to use as one of the most effective solutions to meet these regulations. Furthermore, engine downsizing contributes to less fuel consumption, which is an important challenge in the auto industry as well. However, without taking advantage of a turbocharger (TC), the small engines cannot fulfill the performance requirements of the industry. Turbocharging increases the engine's produced output power and torque by effectively increasing the density of the intake air (Heywood 2009). The exhaust gases leaving the engine with relatively high pressure and temperature drive a turbine before being released into the environment. A coaxial compressor uses this recovered work to compress the intake air. This technology is currently being widely used in the auto industry, and its market is expected to grow even more in the near future (Hannibal 2018). Since the thermodynamic constraints limit the achievable maximum pressure ratio of a compressor, multi-stage turbocharging is more common in large engines. However, single-stage turbocharging is still preferred in many cases, owing to its benefits such as lower costs, less weight, smaller installation space, and less complexity (Wiesbaden 2018).

Selecting an appropriate turbocharger with the necessary characteristics to fulfill the designer's required performances in interaction with the engine at different speeds is a complicated process. The compressor's operating conditions must be far enough from the surge line and the choke line at all the operating speeds, and it should work at as high efficiencies as possible. The turbine's characteristics have direct effects on the compressor's working condition, and the engine's performance also varies, depending on the characteristics of these two. Therefore, performance prediction of the components and the selection process should be carried out simultaneously.

A considerable amount of literature has been published on turbocharger matching. Shaabani Jafroudi *et al.* (2010) performed an experimental turbocharger matching process for a naturally aspirated diesel engine to compensate for the reduction of the engine's generated power due to changing the fuel to CNG. They selected a Holset 4LEV turbocharger and suggested the required engine modifications. Their results showed that by using this turbocharger, the engine's generated power could be increased by 25%. However, observing the engine performance by executing empirical tests is too expensive and time-consuming and should only be done at the final stages of the engine design or turbocharger selection. Similarly, simulating the system using CFD software may not be convenient at the initial stages of the design or selection process.

It is common to select the turbocharger by the trial-and-error method using engine 1D simulation software such as GT-power and AVL Boost and empirical data maps of the turbine and the compressor provided by their manufacturers. In a study by Sajedin (2010), two suitable turbochargers for a SI engine were chosen, regarding compressor performance and the engine's target power and using commonly used matching methods. The engine's performance equipped with each of the turbochargers was then simulated in GT-power software, and results such as compressor efficiencies, brake torque, and turbocharger shaft speed have been compared. The effects of spark timing and valve timing have been studied, and some modifications have been suggested. Studying wastegate mass flow rates, she suggested that more bypassed exhaust gases before the turbine are preferable in similar performances due to faster system responses. Ghazikhani *et al.* (2014) investigated the enhancement of a naturally aspirated 6-cylinder gasoline SI engine by adding a turbocharger. The engine was modeled in GT-power software, and the model was validated with experimental test results of the engine. Using instructions provided by turbocharger manufacturers, they selected GT2052 and upgraded the GT-power model with this turbocharger. Simulating the turbocharged engine and making some modifications such as changing the exhaust manifold and adding an intercooler, they compared the turbocharged engine with the first engine. They concluded that making these modifications will result in a 26% increase in the engine's maximum brake power and a 30% increase in its maximum torque. Mahmoudi *et al*. (2017) also used GT-power to research the effects of turbocharging a 3L gasoline engine on emission levels. Validation of the simulation results was proved by comparing them with experimental data. The deviation of calculated full-load brake powers in different engine speeds from the corresponding experimental data did not exceed 20.2%. Their results showed that the maximum torque and power of the turbocharged engine could reach 543 Nm (at 4000 rpm) and 371 HP (at 6000 rpm) compared to 275 Nm and 193 HP for the naturally aspirated engine. The turbocharged engine also performed a wider range of near-to-peak power. This increase in power was followed by more fuel consumption and, therefore, more emission concentrations. Though, the brake specific emission for the turbocharged engine was lower, which confirmed turbocharging as a means to decrease the emission of the engine by the same performance. Motahari and Chitsaz (2019) used GT-power to study the influence of the pressure and temperature of the ambient air on the performance of a turbocharged direct injection gasoline engine. Their results show that for high intake temperatures, the spark time is retarded, resulting in a drop in engine efficiency. Therefore, the torque decreases and BSFC increases. They also concluded that in high altitudes, the knock controller advances the spark

time, which contributes to an increase in engine efficiency. Nevertheless, 1D simulation of the engine also requires too many details, which may not be present before the engine is fully designed. Furthermore, sufficient accuracy for TC-matching may also be possible by 0D models in considerably less time.

Turbocharger manufacturers often provide 0D online simulation programs (e.g., BorgWarner; Matchbot, Garrett; Boost Adviser, etc.), which suggest the appropriate turbocharger among their available products, based on user-specified engine details and target performances. However, these programs do not offer much flexibility, and the results may not be sufficiently accurate and reliable to be used by auto manufacturers or professional individuals. Liu *et al.* (2011) proposed a method for pre-matching an engine with turbocharger and developed a program for the preliminary selection of components. The program was connected with a database containing compressor and turbine maps. Based on mass flow and pressure ratio range, the program determined whether a compressor or a turbine was suitable for the engine or not. The program then suggested all the acceptable models in the database for further simulations in GT-power. The final decision was made based on the results of the GT-power model. An integrated turbocharger design approach was proposed by Zhang *et al.* (2010) to optimize the compressor and turbine design parameters regarding engine specifications and operational requirements. By using this model, it was possible to design the most suitable turbocharger and simultaneously modify engine characteristics, instead of selecting a turbocharger among available products. Turbine and compressor characteristic maps were generated based on their geometrical characteristics and were used in engine performance simulation. Geometry data such as wheel inlet, wheel exit, blade angles, etc. could then be modified until they match performance requirements. In a project between Napier Turbochargers Ltd and the University of Lincoln, Okhuahesogie *et al.* (2012) dealt with the design and optimization of the impeller of a high-pressure compressor in a two-stage turbocharging system. At preliminary stages of the design, a computer program had been developed to calculate the mass flow and component requirements, with known pressure ratios of both compressors and input temperatures of all components. A second program had been developed to analyze the compressor performance and optimize the impeller for a specific working condition. Qiu *et al.* (2013) developed an integrated system that allowed the user to design a new turbocharger and optimize it on a system level, with only basic engine parameters specified. Two mean-line programs were linked to the main program and handled the modeling of the compressor and the turbine. Simple models for EGR, wastegate, and intercooler were used. In the design mode of the program, it calculated the optimized compressor and turbine geometry for given boost pressure and turbocharger speed. In analysis mode, computing of performance of a known turbocharger design was also possible. The program was applied to design a new turbocharger for an 18-cylinder diesel engine. Although optimizing the component geometries for a given condition can be helpful for turbocharger producers, when it comes to the auto industry, the whole working range of the engine must be considered at the same time. A new method for specifying the optimum geometric and aerodynamic design characteristics of the turbocharger components for a specific engine was proposed and used in computer code by Sanaye *et al.* (2015) In this method, the compressor, the engine, and the turbine performances were modeled employing thermodynamic and turbomachinery analyses. Optimization constraints were also suggested and discussed in the study. By using a genetic algorithm, the code designed the optimum turbocharger so that the sum of losses in the compressor and the turbine was minimum. An appropriate position of the operating point of the turbocharged engine on the compressor map was also an important constraint. A dimensionless parameter was defined to evaluate the distance of a point from the surge and choke line. The geometric variables of the turbocharger, such as the blade tip radiuses and the blade tip angles, the number of blades, and the area-to-radius (A/R) ratio of the turbine, were reported as the output of this code. Moslemzadeh *et al.* (2014) proposed an algorithm for simulating the Wankel engines and wrote a computer program to study the possibility and the effects of using a turbocharger on these engines. They compared the engine's performance on both turbocharged and naturally aspirated conditions with different intake pressures. Their results showed that the engine's brake specific power could be increased by 38% by turbocharging. Though, the brake specific fuel consumption is reduced only for engine speeds over 5500 rpm. An analytical method for turbocharger selection based on characteristic maps of the components is proposed and validated by Lakhlani (2017). The turbine inlet temperature is estimated by the first law of thermodynamics, and the wastegate fraction and EGR fraction are provided by the user. Agha Seyed Mirzabozorg *et al.* (2018) wrote a C-programming code that suggested the optimum turbocharger combination (among its available turbocharger database) for a propulsion system for aerial application, knowing the altitude and the target power of the engine. The proposed system included the number and model of the turbochargers and also the number of required intercoolers. The optimization was based on the maximum power and maximum speed of the engine. The code initially checked if this working point was within the allowable region on the compressor map, then suggested the appropriate turbocharger(s), based on multiple defined criteria. Mizythras *et al.* (2019) implemented 0D modeling for developing a methodology for matching turbochargers to a marine two-stroke diesel engine. The methodology is implemented for a vessel propulsion engine. Selecting the optimum turbocharger, the engine fuel consumption is reduced by 2-4% at different engine loads. Yang *et*

al. (2019) proposed a guideline for matching an electric turbo compound to reach an optimum engine fuel economy. They studied the effect of the power produced by the electric generator and the turbocharger efficiency on the engine efficiency, concluding that the turbocharger efficiency is the most important factor. They implemented the guideline on a two-stroke low-speed diesel engine, and reduced the brake specific fuel consumption (BSFC) of the engine by about 2-3%.

By looking through the previous literature, a lack of a convenient zero-dimensional engine simulation method for predicting the performance of turbocharged internal combustion engines with various compressors and turbines seems to exist. Hence, the main aim of the current work was to develop an integrated, flexible TC-matching program that comes in use in every stage of engine development. Since the TC-matching process is mostly performed in the early stages, one of the primary aims of this work was to give the user the possibility of simulating the system with limited information, as well as the option of modeling the details of the engine (e.g., geometry, fuel, valve timing, etc.) for more accurate results. Using the algorithm described in this paper, modeling both wastegated and free-floating turbines is possible with only a small change in the process. The effects of using a wastegated turbine housing are also considered and discussed. In cooperation with a database, the program gives the designer the possibility to predict the engine's performance in interaction with a variety of compressor-turbine combinations in a particularly short time and to choose the best combination by comparing the results together. The validity of the discussed methods is verified by comparisons with an existing turbocharged engine's experimental results, obtained from testing it on an engine test bench. Finally, two other compressor-turbine combinations are found for the same engine, and their performances have been evaluated.

2. SIMULATION METHOD

In this section, the method of modeling each component (the compressor, the turbine, and the engine) is described. Subsequently, the thermodynamic relations and the algorithm of simulating the interaction between the components are explained.

2.1 Compressor and Turbine Maps

A typical compressor characteristic map is illustrated in Fig. 1. The turbine's characteristic map includes two diagrams, which are shown in Fig. 2 and Fig. 3. In both maps, the corrected (or similar) mass flow rate and the efficiency of the component are linked to the pressure ratio (P_2/P_1 for the compressor map and P_4/P_5 for the turbine map) for different shaft speeds. The corrected mass flow rate (ASME standard) for both components is defined in Eq. (1), whereas the similar mass flow rate (SAE standard) is defined in Eq. (2). Similarly, the corrected shaft speed is defined in Eq. (3), and the similar shaft speed in Eq. (4).

$$\dot{m}_{corr} = \dot{m}\frac{\sqrt{T_{in}/T_{ref}}}{P_{in}/P_{ref}} \tag{1}$$

$$\dot{m}_{corr} = \dot{m}\sqrt{T_{in}}/P_{in} \tag{2}$$

$$N_{corr} = \frac{N_{shaft}}{\sqrt{T_{in}/T_{ref}}} \tag{3}$$

$$N_{corr} = N_{shaft}/\sqrt{T_{in}} \tag{4}$$

where P_{ref} and T_{ref} are the reference pressure and the reference temperature, P_{in} and T_{in} are the input pressure and the input temperature (P_1 and T_1 for the compressor, and P_4 and T_4 for the turbine), N_{shaft} is the shaft speed of the turbocharger, and N_{corr} is the corrected shaft speed of the turbocharger.

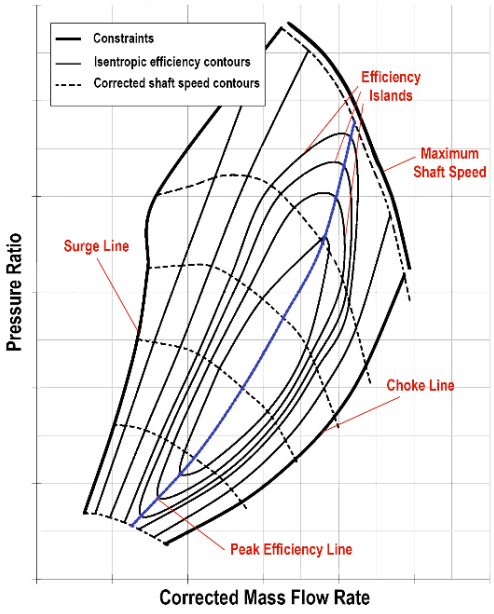

Fig. 1. A typical compressor map.

The dashed curves in Fig. 1 represent constant corrected shaft speeds, and the solid curves represent isentropic efficiency contours of the compressor (η_c). The peak efficiency line represents the point at every shaft speed in which the compressor works with its maximum isentropic efficiency. The compressor map is restricted with the surge line from the left, the choke line from the right, and the maximum shaft speed from above.

In turbine characteristic maps, it is common to present the corrected mass flow rate and the turbine-mechanical efficiency in separately. In Fig. 2 and Fig. 3, each curve is associated with a turbine shaft speed. Due to friction and heat release, a part of the work produced by the turbine does not reach the compressor. Mechanical efficiency of the turbocharger will be defined as the ratio of the compressor's work rate to the turbine's work rate

($\eta_m = \dot{W}_c/\dot{W}_t$). Turbine's isentropic efficiency multiplied by the turbocharger's mechanical efficiency is called turbine-mechanical efficiency ($\eta_{tm} = \eta_t\eta_m$) and is also provided on the turbine map (Fig. 3).

A database containing digitized maps of 48 compressors and 20 turbines (provided by their producers in Garrett Advancing Motion 2019, and BorgWarner 2017) is created for this work and is integrated into the program. Information such as the reference pressure and the reference temperature, the correction standard of the mass flow rate and the shaft speed (SAE or ASME), the maximum allowable speed, and the geometry are also included. Before beginning the simulation, the program reads the associated maps and details to the models identified by the user from the database and uses them to predict the working conditions of the turbine and the compressor.

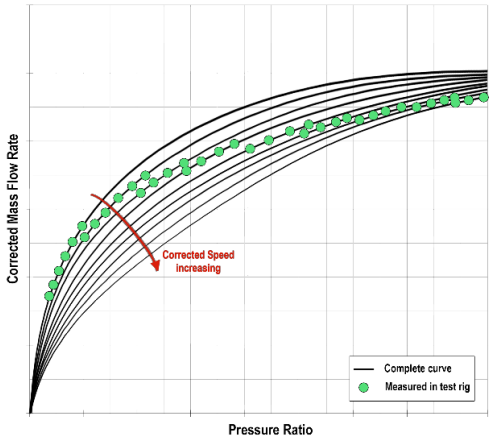

Fig. 2. A typical turbine map (part 1).

2.2 Interpolating and Extrapolating

One of the problems with using characteristic maps is inter- and extrapolating them. Due to the special conditions of the turbocharger test rigs, at each shaft speed, only a limited turbine pressure ratio range could be reached, while other pressure ratios might also be met if the turbine is tested separately. This is evident in comparing the green dots to the solid curves in Figs. 2 and 3. This phenomenon intensifies the necessity of using a robust method for extrapolating the turbine maps even more. For this reason, four physical-based algorithms for interpolating and extrapolating have been employed, all described in detail in El Hadef *et al.* (2012). In characteristic maps provided by turbocharger manufacturers, there are usually at least six rotational speeds, each with eight points, which is sufficient for using these algorithms. Methods and equations used for inter- and extrapolating the data maps are briefly described in this section.

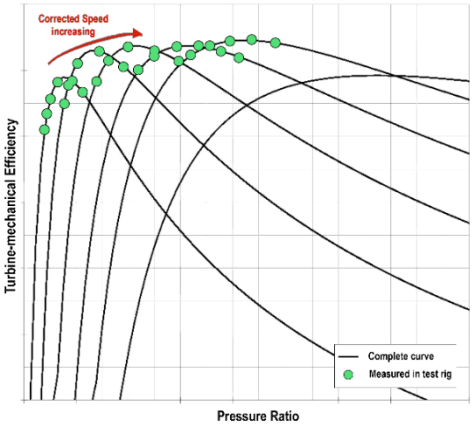

Fig. 3. A typical turbine map (part 2).

I. COMPRESSOR ROTATIONAL SPEED

The objective is to develop a model to predict the compressor's rotational speed, having its pressure ratio and mass flow rate. However, El Hadef *et al.* (2012) represent a model to predict the pressure ratio, having the mass flow rate and the rotational speed. The strategy was to

use this model and calculate pressure ratios for different speeds (and a fixed mass flow rate) until the calculated pressure ratio matches our known value.

The model is based on two dimensionless parameters: the head parameter (ψ) and the dimensionless flow rate (ϕ), which are related by Eq. (7).

$$\psi = \frac{C_p T_{in}\left[\left(\frac{P_{out}}{P_{in}}\right)^{\frac{\gamma-1}{\gamma}} - 1\right]}{\frac{1}{2}U_c^2} \tag{5}$$

$$\phi = \frac{\dot{m}}{\rho\frac{\pi}{4}D_c^2 U_c} \tag{6}$$

$$\psi = \frac{A + B\phi}{C - \phi} \tag{7}$$

where P_{out} is the outlet pressure, U_c is the blade tip speed, and D_c is the wheel diameter of the compressor. A, B, and C are identified based on the available data points. A second-order polynomial is fitted for each of them with respect to the rotational speed.

II. TURBINE MASS FLOW RATE

The mass flow rate of the turbine is predicted by a parameter called equivalent area (S_{Mach}), defined in Eq. (8), where V_{Mach} is a function of the flow Mach number, defined in Eq. (9).

$$S_{Mach} = \frac{\dot{m}_{corr}}{V_{Mach}}$$

$$\begin{cases} V_{Mach} = \sqrt{\frac{\gamma}{R}}\left(\frac{2}{\gamma+1}\right)^{\left(\frac{\gamma+1}{2\gamma-2}\right)} & \text{if } M_a > 1 \\ V_{Mach} = \sqrt{\frac{\gamma}{R}}\frac{M_a}{\left(1+\frac{(\gamma-1)M_a^2}{2}\right)^{-\left(\frac{\gamma+1}{2\gamma-2}\right)}} & \text{otherwise.} \end{cases}$$

For each available data point, S_{Mach} is calculated. It is then modeled as Eq. (10), where k_1 and k_2 are constants. They are determined for each available speed and then extrapolated as second-order polynomials with respect to the rotational speed.

$$S_{Mach} = k_1\left[1 - exp\left(1 - \frac{P_{out}}{P_{in}}\right)^{k_2}\right] \quad (10)$$

III. ISENTROPIC EFFICIENCY

The methodology for predicting the isentropic efficiency is similar for both components. First, the isentropic specific enthalpy exchange (Δh_{is}) is calculated for available data points using Eq. (11). Having the isentropic efficiency, the specific enthalpy exchange (Δh) is then determined by definition for each data point. In Eq. (12), a and b are determined for each rotational speed. Afterward, they are extrapolated with a second-order polynomial with respect to the rotational speed.

$$\Delta h_{is} = \left|\left(\frac{P_{out}}{P_{in}}\right)^{\frac{\gamma-1}{\gamma}} - 1\right| C_p T_{in} \quad (11)$$

$$\Delta h = a + b\,\dot{m}_{corr} \quad (12)$$

For any given point, first, a and b are determined using the fitted polynomials. Then Δh_{is} and Δh are calculated using Eq. (11) and Eq. (12). The ratio of these values could determine the isentropic efficiency.

2.3 Modeling The Engine

The TC-matching process is often carried out before the engine is produced or even fully designed. Hence, there might be little information about the details of the engine. On the other hand, one of the deciding parameters affecting the entire simulation is the temperature of the gases leaving the engine (EGT). In fact, errors higher than 100 Kelvin in EGT lead to an inadequate accuracy of the final results. By modifying the engine simulation

codes provided by Ferguson and Kirkpatrick (2015), two sub-programs are developed and integrated into the program to calculate the EGT. However, if the EGT is known, it is highly recommended to provide it directly as an input parameter.

One of the sub-programs treats the engine as an ideal four-stroke Otto fuel-air cycle, requiring only the compression ratio and the fuel type of the engine, and a few other parameters (inlet pressure and temperature, output pressure, air-fuel ratio) which are calculated at this stage of the simulation. The sub-program iterates related thermodynamic equations (Ferguson and Kirkpatrick 2015), updating thermodynamic properties and the initial guesses each time until they are all converged.

The other sub-program considers details such as cylinder geometry, valve timing, combustion timing, residual fraction (which is converged through the engine model), cylinder temperature, and heat transfer coefficient between the gases and the cylinder to calculate a more realistic EGT. This sub-program updates the cylinder geometry and integrates the differences in properties through each crankshaft angle at the compression and the combustion strokes, then updates the assumed parameters and repeats the procedure until they are converged.

Utilizing functions available in Ferguson and Kirkpatrick (2015), fluid properties and fuel characteristics are determined throughout the entire simulation. Each of the following can be selected as the engine's working fluid before the simulation starts: 1. Gasoline, 2. Diesel, 3. Methane, 4. Methanol, and 5. Nitromethane.

2.4 System Interactions and Relations

The general procedure of simulating the system will be described in this section. The required parameters before starting the matching process are listed in Table 1. The simulation is carried out for the full load engine conditions since it is sufficient for the initial matching of the compressor and the turbine, as described in Baines (2005). Hence, the parameters of Table 1 should be provided for the full load condition. If one of the engine models are used, additional engine details (instead of EGT) are required. In the case of a wastegated turbine, one of the following must be determined as the restriction: 1. Compressor outlet pressure, 2. Compressor pressure ratio (PRC), 3. Pressure difference between inlet and outlet of the compressor, and 4. Engine inlet pressure. If the turbine is free-floating, none of them is needed. The equations in this section are from Baines (2005).

The compressor, the intercooler, the engine, and the turbine are considered as a series of interconnected

components, as illustrated in Fig. 4. Mean values are considered for all pressures and temperatures. Air with ambient pressure and temperature passes the air filter before entering the compressor. Temperature difference through the air filter is neglected ($T_1 = T_{amb}$). Air pressure at stage 1 (compressor inlet) is determined by

$$P_1 = P_{amb} - P_{d,AF} \quad (13)$$

The compressor outlet temperature is evaluated from the definition of the compressor's isentropic efficiency by Eq. (14), where η_c is the isentropic efficiency of the compressor and γ_a is the heat capacity ratio of the air.

$$T_2 = T_1\left\{1+\frac{1}{\eta_c}\left[\left(\frac{P_2}{P_1}\right)^{\frac{\gamma_a-1}{\gamma_a}}-1\right]\right\} \tag{14}$$

Table 1 List of required input data.

P_{amb}	Ambient Pressure
T_{amb}	Ambient Temperature
N	Crankshaft speed
$BSFC$	Brake specific fuel consumption of the engine
V_{eng}	Engine displacement volume
P_{eng}	Engine's target output power
η_{vol}	Engine's volumetric efficiency
T_{IC}	Coolant temperature
ε_{IC}	Intercooler effectiveness
$P_{d,AF}$	Pressure drop through the air filter
$P_{d,IC}$	Pressure drop through the intercooler
$P_{d,muff}$	Pressure drop through the muffler
T_4	Exhaust manifold temperature

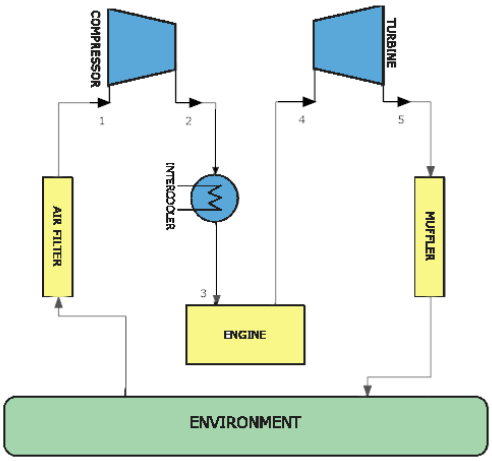

Fig. 4. Schematic of a turbocharged internal combustion engine.

Pressure and temperature at stage 3 (engine inlet) are evaluated by

$$P_3 = P_2 - P_{d,IC} \tag{15}$$

$$T_3 = T_2\left(1-\varepsilon_{IC}\right)+T_{IC}\varepsilon_{IC} \tag{16}$$

Assuming that air behaves as an ideal gas, air mass flow rate ($\frac{kg}{s}$) through a 4-stroke engine can be calculated by Eq. (17), where N_{eng} is the number of crankshaft revolutions per minute, P_3 is inlet manifold pressure (kPa), R_a is the gas constant of air ($\frac{kJ}{kgK}$), V_{eng} is engine displacement (L), and η_{vol} is the volumetric efficiency of the engine.

$$\dot{m}_a = \left(\frac{N_{eng}}{120}\right)\frac{P_3}{R_a T_3}\frac{V_{eng}\eta_{vol}}{1000} \tag{17}$$

Fuel mass flow rate is calculated by the definition of the brake specific fuel consumption.

$$\dot{m}_f = BSFC \times \dot{W}_{eng} \tag{18}$$

$$\left[\left(\frac{P_2}{P_1}\right)^{\frac{\gamma_a-1}{\gamma_a}}-1\right]C_{p,a}T_1 = \left[1-\left(\frac{P_5}{P_4}\right)^{\frac{\gamma_e-1}{\gamma_e}}\right]C_{p,e}T_4\left(\frac{\dot{m}_t}{\dot{m}_a}\right)\eta_t\eta_m\eta_c \tag{19}$$

Regarding the fact that the turbine supplies the compressor's required work, the energy balance between these components gives Eq. (19), where $\dot{m}_t$ is the mass flow rate through the turbine, η_{tm} is the turbine-mechanical efficiency, and $C_{p,a}$ is the specific heat of the air at constant pressure ($\frac{kJ}{kgK}$).

The turbine's output pressure is determined by

$$P_5 = P_{amb} + P_{d,muff} \tag{20}$$

In the case of a wastegated turbine, a portion of the exhaust gas bypasses the turbine wheel. Thus, the mass flow rate through the turbine wheel can be calculated as in Eq. (21), where y is the bypassed mass flow rate percentage. If the turbine is not equipped with a wastegate, y always equals zero.

$$\dot{m}_t = (1-y)(\dot{m}_a + \dot{m}_f) \tag{21}$$

Due to additional friction and flow changes caused by the wastegate, the isentropic efficiency of the turbine, thus the turbine-mechanical efficiency, reduces continuously with the opening of the wastegate for wastegate angles less than 20 degrees, as suggested in Capobianco and Marelli (2007). In wastegate angles more than 20 degrees, the efficiency drop starts to increase. However, the results of a study by Alaviyoun *et al.* (2020) show that the wastegate angle does not exceed 6 degrees in normal working conditions. Analyzing the experimental data available in Capobianco and Marelli (2007), Eq. (22) is derived for modeling the efficiency reduction, where η_{tm} is the actual turbine-mechanical efficiency, and η'_{tm} is the associated turbine-mechanical efficiency from the turbine map

$$\eta_{tm} = \eta'_{tm} \times \exp(0.0616y) \tag{22}$$

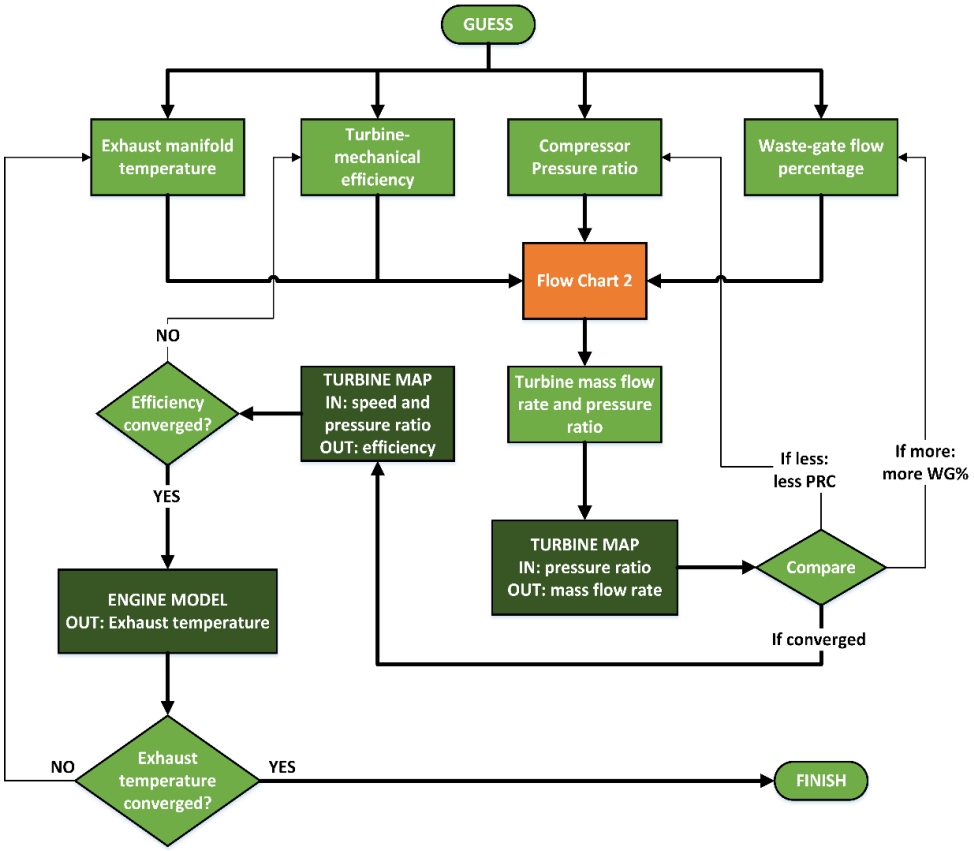

Fig. 5. Basic Flow chart for the iterations.

Using compressor and turbine maps and one of the engine models (or known EGT), the program iterates Eq. (13) to Eq. (22) to simulate the whole system. The flowchart of the main iteration loops is illustrated in Fig. 5. Initially, estimated values of four parameters (specified as guesses) are employed for executing the equations, and then, by comparing the results with the ones from the models of each component (the compressor, the turbine, and the engine), each of these parameters is modified in a loop. The whole process repeats until all of the estimated parameters are converged. The wastegate percentage and PRC are converged in the first loop. The restricted quantity by the user will determine the first guess for PRC (upper limit). Assuming this value for PRC, the pressure ratio of the turbine (PRT) and the mass flow rate through the turbine are calculated. Referring to the turbine map, the corresponding mass flow rate to the calculated PRT is determined as well. As indicated in Fig. 5, the wastegate percentage and the PRC are modified until the two mass flow rates match. For free-floating turbochargers, either the user puts an upper limit PRC, or instead of increasing the wastegate percentage, the program increases PRC.

Subsequently, the program refers to the turbine map once again to update the assumed turbine-mechanical efficiency in an outer loop. A vital characteristic of the system is used here: the actual rotational speed of the turbine and the compressor must be the same. The associated turbine-mechanical efficiency to the determined rotational speed of the turbocharger and the calculated PRT (from Eq. (19)) is read and updated until it is converged. If an engine model is used, the calculated parameters in previous steps are used to estimate a new EGT. The entire process is repeated with this new EGT until it converges too. Since the engine modeling is the most time-consuming part of the process, it has been settled as the last loop in order to decrease the number of its iterations, hence, the running time of the whole program. The details and order of applying the equations are depicted in Fig. 6. Finally, the calculated working conditions of the compressor and the turbine will be plotted on their maps and reported to the user.

3. CASE STUDY

A 1.65L turbocharged gasoline engine, the technical information of which is listed in Table 2, was tested under different working conditions, and the experimental results were obtained. The program was then employed to simulate the performance of the same engine under the same conditions as in the experiments. The compressor map, and the turbine map, provided by the Iran Khodro Powertrain Company (IPCO), were used in the simulation. The simulation has been carried out for seven working conditions, once with known EGT and once with calculating EGT using engine sub-programs. In order to verify the results of the program, these are compared with the test results and are discussed in the following sections.

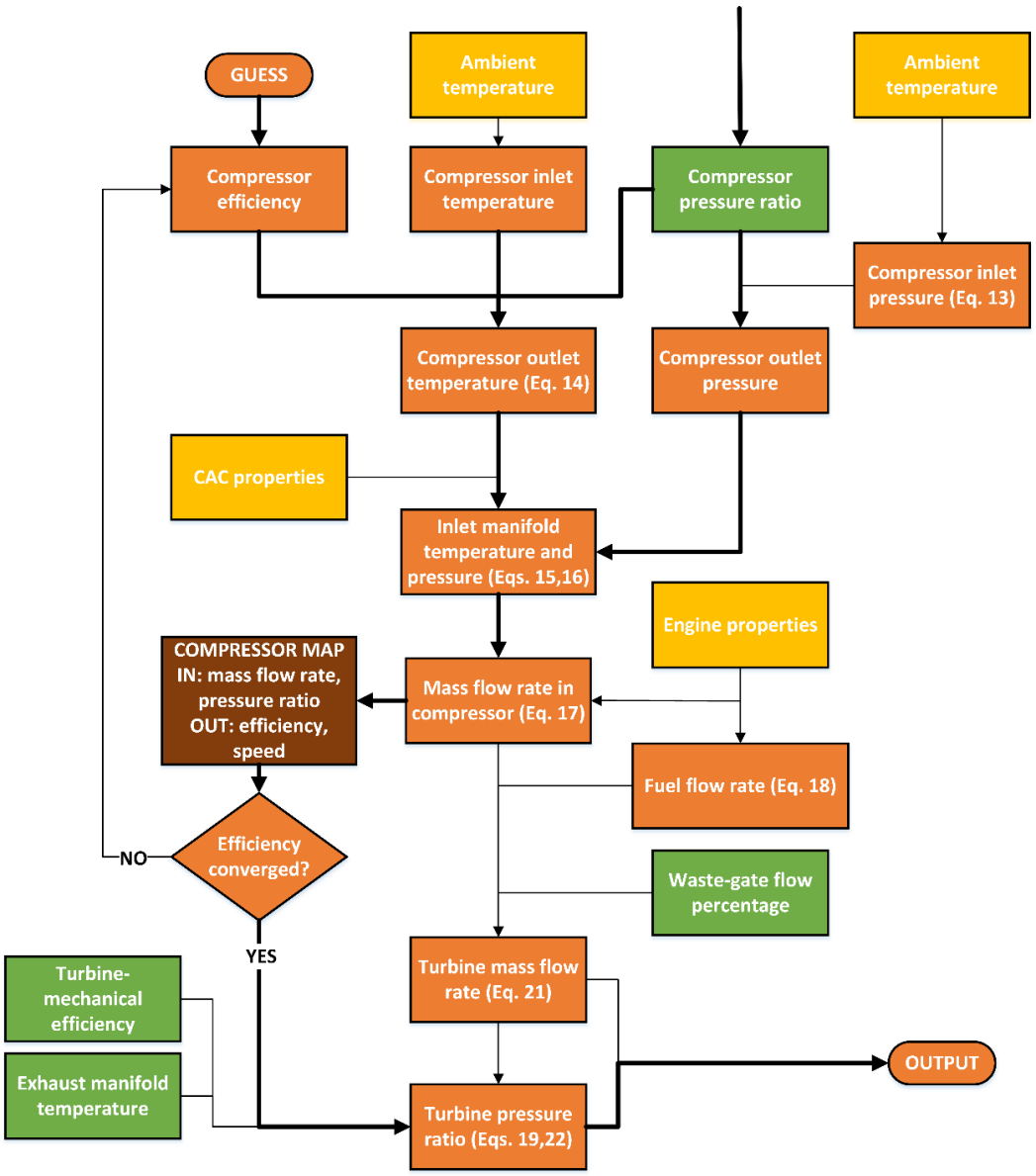

Fig. 6. Flow chart for calculating details.

3.1 Experimental Results

Investigating a turbocharged engine requires comparably high-accuracy measurements across the turbocharger components and the engine. The experimental task has been performed on a standard engine test bench at IPCO. The engine parameters and mass flows, temperatures, and pressures are measured at the inlet and the outlet of the compressor, and the turbine housing. In addition, the turbocharger rotational speed and the wastegate arm opening have been measured in different working points of the engine. Experimental results show that the wastegate is completely closed at 1500 rpm and full load condition. The measurement range of the temperature sensor was -200°C to 1200°C, and the accuracy was ±2°C. Moreover, the measurement range and the accuracy of the pressure sensor were 0 to 2.5bar gauge and ±2.5kPa, respectively. Different tests have been performed on full load conditions at different engine speeds. Also, each test has been repeated three times to check the repeatability of the experiment. Figure 7 shows the engine test bench during the experiments.

Table 2 Engine characteristics.

Number of Cylinders	4
Volume	1.65L
Bore	79mm
Stroke	85mm
Compression Ratio	9.3:1
Rated Power	120kW @5500rpm
Maximum Torque	240Nm @4000rpm

Fig. 7. Turbocharged engine on the test bench during the experiments (courtesy of IPCO).

3.2 Comparison of the Results

The comparisons between the program predictions and engine test results for the full load conditions are illustrated in Figs. 8 through 15. Green points correspond to the results of the experimental test. Blue points correspond to the results of the simulation when the second engine model is employed for predicting the EGT. Yellow points correspond to the results of the simulation when known values of EGT (from the experiment) are provided as inputs. In Fig. 14, which shows the EGT, yellow points correspond to the results of the simulation with the first engine model. Altogether, both simulations agree with the test results quite well and adequately for TC-matching purposes. The results of the two simulations could be compared together in order to evaluate the effect of errors in EGT on other parameters.

To evaluate the accuracy of the whole matching results briefly, one can evaluate only pressure ratios of the compressor and the turbine, which actually represent the calculated pressures at the compressor outlet (P_2), and at the turbine inlet (P_4), since the pressures at the compressor inlet (P_1) and at the turbine outlet (P_5) are indirectly (Eq. (13) and Eq. (20)) known through pressure drops. As depicted in Fig. 8 and Fig. 9, these two follow the trend of the test results quite well and differ only slightly by a 16% maximum error in the turbine pressure ratio at 6000rpm crankshaft speed. It is notable that the compressor pressure ratios for engine speeds higher than 2000 are almost identical, since the engine inlet pressure (P_3) is restricted by the wastegate.

The air mass flow rates (Fig. 10) of both simulations

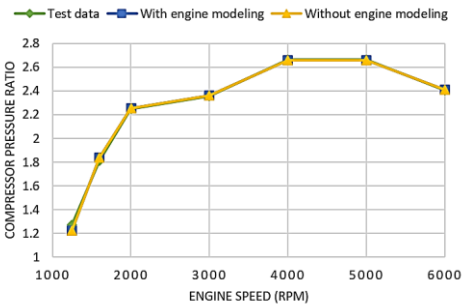

Fig. 8. Compressor pressure ratio comparison.

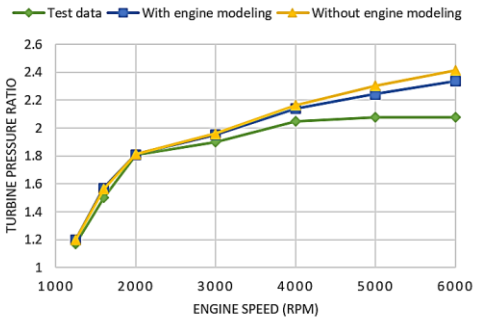

Fig. 9. Turbine pressure ratio comparison.

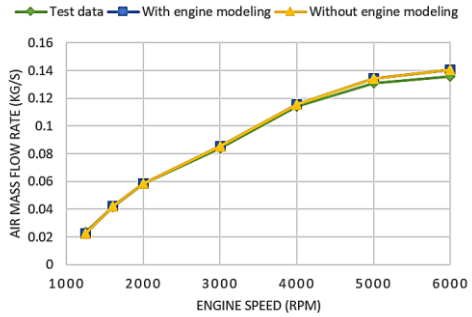

Fig. 10. Air mass flow rate comparison.

agree with the test results almost precisely, indicating that Eq. (17) works out effectively. Similarly, Eq. (18) is validated through the high accuracies of air-to-fuel ratios, as Fig. 11 depicts. Figure 12 shows the compressor output temperature (T_2) calculated from Eq. (14) in each simulation, the maximum difference of which with the test results is 27K. This deviation is actually associated with the error of the compressor's isentropic efficiency (Fig. 13) in the last two engine speeds. The maximum relative error in compressor efficiency is 5%, again at 6000rpm. However, this error does not exceed 2% in the other five engine speeds.

As depicted in Fig. 14, the EGT is calculated with a maximum error of 55K (10K for the first five engine speeds). The fact that the results of both simulations, with engine modeling and with previously known EGT, are almost identical suggests that this accuracy is sufficient for TC-matching purposes, and the engine model can be trusted. The results of the ideal engine modeling are also included in Fig. 14, which

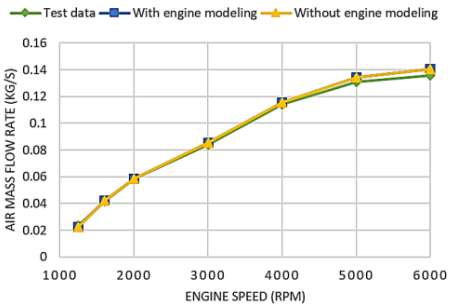

Fig. 11. Air to fuel ratio comparison.

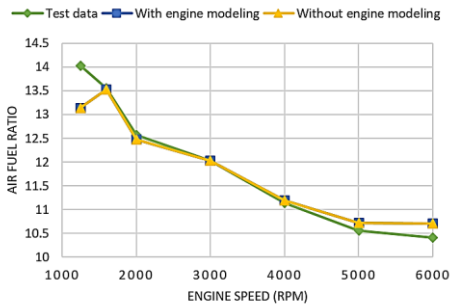

Fig. 12. Compressor output temperature comparison.

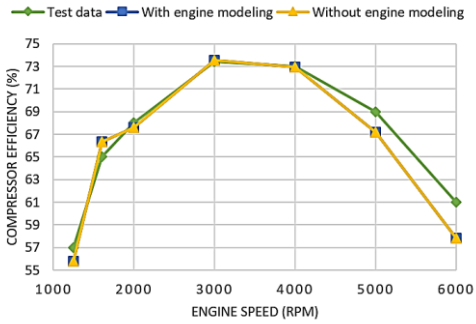

Fig. 13. Compressor efficiency comparison.

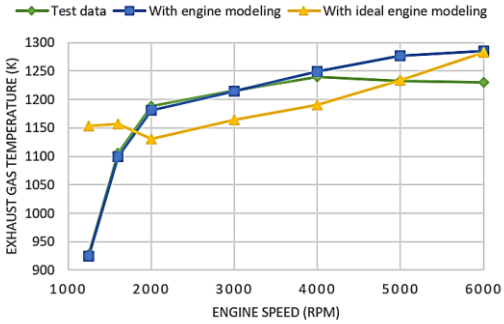

Fig. 14. Exhaust gas temperature comparison.

indicates that the ideal model cannot be trusted in low engine speeds. However, except for the lowest engine speed, the results are deviated by less than 60K. When detailed characteristics of the engine are not available, the ideal model could come useful. The estimated turbocharger shaft speed of both simulations (Fig. 15) are also nearly identical and differ from the test results by a maximum error of 13%.

The simulated operating conditions of the compressor are plotted on its characteristic map and reported to the user, as depicted in Fig. 16. This plot shows that the compressor works suitably with this engine and this turbine since all of the points are between the surge margin and the choke margin, and none of them exceeds the allowable speed. The simulation's total run time for seven engine speeds was less than 200 seconds with engine modeling and less than 10 seconds with known EGT.

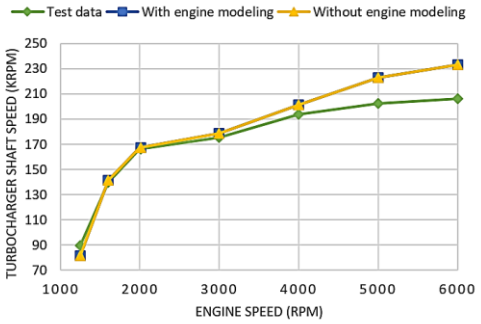

Fig. 15. Turbocharger shaft speed comparison.

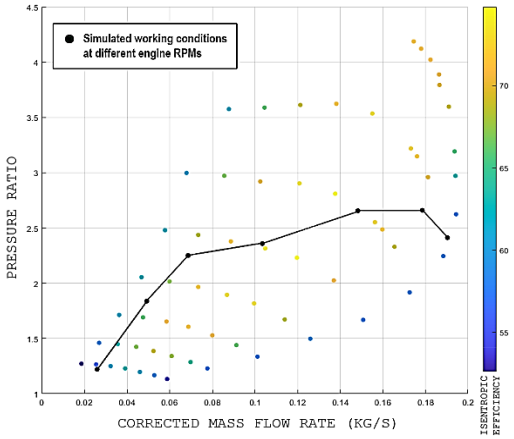

Fig. 16. Simulated working conditions plotted on the compressor map.

4. SELECTING A TURBOCHARGER

The program could be implemented to predict the working condition of different compressor-turbine combinations with a specific engine in a short time. Evaluating the results, the designer initially dismisses the combinations that do not satisfy the limitations of the components. Subsequently, the designer compares the working conditions of the remaining combinations and selects several of them based on the criteria suggested in the following. These combinations are then tested experimentally for the final decision.

In this section, the limitations of the components and the criteria for selecting a turbocharger are discussed. Using the available characteristic maps in the database, other combinations are simulated for the studied engine, and one of them is suggested as an alternative turbocharger.

4.1 Component Limitations

As indicated in Fig. 1, the compressor must remain within a mass flow range at each turbocharger shaft speed. This is especially important at low engine speeds where the compressor may enter the surge

zone, and at high engine speeds, where it may not tolerate the entering mass flow rate and get choked. Fig. 17 represents a case where the compressor is choked at high engine speeds, although it works properly at low and moderate speeds.

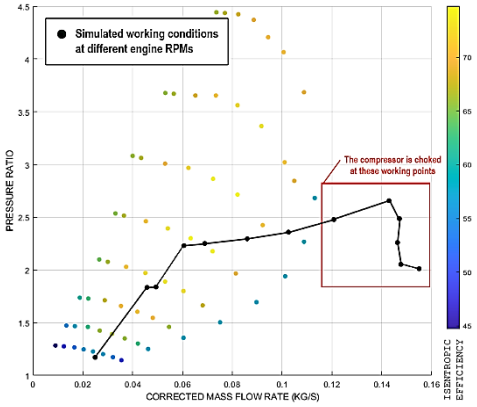

Fig. 17. Simulated working conditions plotted on the compressor map (choked).

Both components are restricted with a maximum shaft speed (normally between 150 and 250 krpm), which may be exceeded if they are not appropriately selected. Another restricting parameter for the turbine is its inlet temperature (EGT). Based on the turbine blades' material, the maximum permissible turbine inlet temperature varies. Exposing the blades to high temperatures results in severe damage and deformation over time. The maximum EGT is around 1000 K for diesel engines and 1250 K for petrol engines (Feneley *et al.* 2017).

4.2 Selection Criteria

An alternative compressor for the turbocharger of the studied engine is simulated with two turbines. The details of the components are listed in Table 3. Both combinations satisfy the limitations of the components discussed above. Various factors could be considered for deciding among these combinations:

Table 3 Details of the turbocharger components.

	Wheel Diameter	Trim	A/R
Initial Turbocharger			
Compressor	46mm	62	0.39
Turbine	39mm	79	0.5
Alternative 1			
Compressor	46mm	54	0.39
Turbine	35.5mm	79	0.27
Alternative 2			
Compressor	46mm	54	0.39
Turbine	39mm	79	0.4

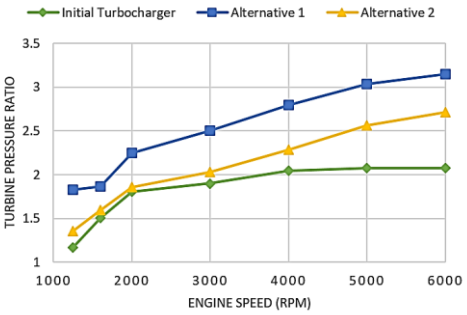

Fig. 18. Simulated turbine pressure ratios of each turbocharger.

1. Smaller A/R ratio of the turbine is advantageous in decreasing the turbocharger's response time (turbo lag). However, it increases the engine back pressure, which is not favorable (Feneley *et al.* 2017). Figure 18 compares the PRT of the three combinations. Considering that the turbine outlet pressure is fixed, it is evident that alternative 1 produces higher engine back pressure (turbine inlet).

2. Efficiencies of both components is another deciding parameter in selecting a turbocharger. Figure 19 shows the simulated compressor efficiencies. The new compressor works better at low crankshaft speeds. However, the efficiency dramatically drops at high crankshaft speeds since the mass flow rate approaches the choke limit. Turbine-mechanical efficiencies are compared in Fig. 20. It is evident that the turbine of alternative 1 performs poorly in this combination and should be dismissed.

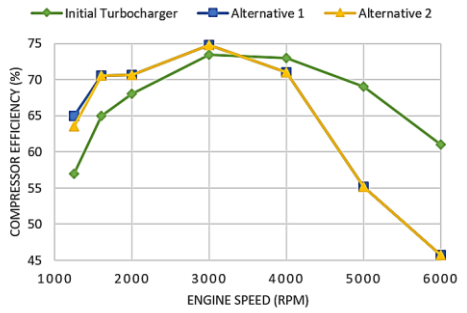

Fig. 19. Simulated compressor efficiencies of each turbocharger.

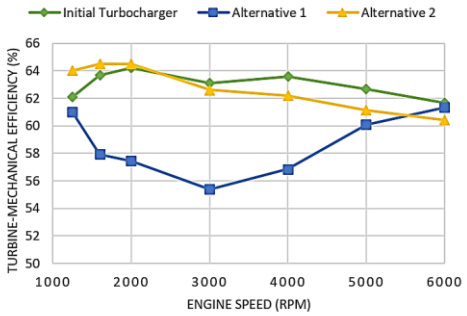

Fig. 20. Simulated turbine-mechanical efficiencies of each turbocharger.

3. The influence of the ambient conditions on the turbocharger's performance could also be investigated and considered in filtering the combinations. The turbocharger must be applicable not only for a wide range of ambient temperatures (which varies during the year and in different areas) but also for various ambient pressures at different altitudes. The importance of altitude change considerably intensifies in TC-matching for aerial applications and has been the subject of many studies (e.g., Roueini *et al*. 2020, Mansouri and Ommi 2019). In a study by Yang *et al*. (2018), the effect of altitude on the performance of a heavy-duty diesel engine and the adaptability of several single-stage turbocharging systems has been explored.

4. Other deciding factors include the emission level (Mahmoudi *et al*. 2017), the peak cylinder pressure, and the combustion zone temperature, which have been discussed in Emara *et al*. (2016). Such criteria are usually evaluated in further examinations (whether by detailed simulation of the engine or by experiment).

Based on the application of the automobile or the company's policies, other criteria may also be considered. The designer prioritizes the criteria and makes the final decision based on further experimental results. A common practice is optimizing the engine for moderate crankshaft speeds since the engine works mostly at these speeds.

5. CONCLUSION

A new algorithm for turbocharger matching has been suggested and employed to develop an integrated turbocharger matching program. Combined with a database containing compressor and turbine maps, this program allows the user to examine the performance of different turbocharger combinations in conjunction with a specified engine. Two engine models have been provided that can be employed if the engine design is still in preliminary stages. Wastegated turbine housing can also be included in the simulation process, and its effect on the turbine-mechanical efficiency is also considered. An existing turbocharged engine has been experimentally tested and also simulated by the program. The program is verified by comparing its results to experimental results. Although the validation has been carried out with a gasoline engine, the program can also be employed for four other fuels. The maximum relative errors for crucial parameters are shown in Table 4. The accuracy of the engine model is validated through the accordance between the results of two simulations. The simulation's total runtime with the second engine model was less than 200 seconds, meaning that evaluating the performance with 100 different compressor-turbine combinations takes less than 6 hours.

The accuracy of the results shows that zero-dimensional simulation with quasi-steady assumptions could be adequately implemented for preliminary TC-matching purposes. Filtering out a large number of possible combinations in a short time, the program enables the designer to focus on the remaining options.

Table 4 Relative errors of the results.

Air mass flow rate	4%	Compressor pressure ratio	4%
Air-to-fuel ratio	6%	Turbine pressure ratio	16%
Compressor output temperature	6%	Turbocharger shaft speed	13%
Exhaust gas temperature	1.5%	Compressor isentropic efficiency	5%

Using the program, two other suitable turbocharger combinations are suggested and evaluated. One of the alternative combinations has been eliminated for low turbine efficiencies. In comparison to the initial turbocharger, the other combination (alternative 2) has the advantage of less turbo lag (corresponding to less turbine A/R), but produces higher engine back pressure, especially in high crankshaft speeds. The compressor efficiency of alternative 2 is preferable at low crankshaft speeds but drops at high speeds. Altogether, both combinations are acceptable. Regarding the customer's need, the new combination could be used for better transient responses, while the initial turbocharger produces less engine back pressure and provides more consistent compressor efficiencies.

ACKNOWLEDGMENTS

The authors thank Irankhodro Powertrain Company (IPCO) for providing the experimental equipment for this research.

REFERENCES

Agha Seyed Mirzabozorg, M., S. Kheradmand and A. Roueini (2018). A C-programming code for selecting the optimum turbocharged propulsion system for UAV's TT. *Mdrsjrns* 18(1), 39–50. (in Persian)

Alaviyoun, S. S., M. Ziabasharhagh and M. Farajpoor (2020). Experimental investigation and numerical simulation of gas flow through wastegated turbine of gasoline turbocharger. *Journal of Applied Fluid Mechanics* 13(6), 1835-1845.

Baines, N. C. (2005). *Fundamentals of Turbocharging*. Concepts NREC, White River Junction, VT.

Borgwarner. (2017). *Performance Turbochargers Catalog*. (accessed October 15, 2020).

Capobianco, M. and S. Marelli (2007). Waste-Gate Turbocharging Control in Automotive SI Engines: Effect on Steady and Unsteady Turbine Performance. *SAE Technical Papers* 724, 776–790.

Emara, K., A. Emara, El Sayed and A. Razek (2016). Turbocharger Selection and Matching. *International Journal of Scientific & Engineering Research* 7 (12), 609–15.

El Hadef, J., G. Colin, Y. Chamaillard and V. Talon (2012). Physical-Based Algorithms for Interpolation and Extrapolation of Turbocharger Data Maps. *SAE International Journal of Engines* 5(2), 2012-01–0434.

Feneley, Adam J., Apostolos Pesiridis and Amin Mahmoudzadeh Andwari. (2017). Variable Geometry Turbocharger Technologies for Exhaust Energy Recovery and Boosting-A Review. *Renewable and Sustainable Energy Reviews* 71 (May), 959–75.

Ferguson, C. R. and A. T. Kirkpatrick (2015). *Internal Combustion Engines: Applied Thermoscience*. 3rd ed. Chester: John Wiley and Sons.

Garrett Advancing Motion (2019). Performance Catalog: Turbochargers, Intercoolers, Accessories. (accessed October 15, 2020).

Ghazikhani, M., M. Falahati and M. Torkamani (2014). Simulating and Turbocharger Selecting for Nissan Engine Considering Pressure Ratio Changes. *The 1st National Conference on Development of Civil Engineering, Architecture, Electricity and Mechanical* in Iran, Gilan, Iran. (in Persian)

Hannibal, W. (2018). Turbocharging Perspective. *MTZ Worldwide* 79(5), 76–76.

Heywood, J. B. and O. Z. Welling (2009). Trends in Performance Characteristics of Modern Automobile SI and Diesel Engines. *SAE International Journal of Engines* 2(1), 2009-01–1892.

Lakhlani, H. (2017). Turbocharger Selection in HD BSIV EGR Engine with the Help of Analytical Method and Correlation with Actual Testing. *SAE Technical Paper* 2017-01-7007.

Liu, J., Z. Zhao, X. Xu, X. Xia and J. Fu (2011). A method on pre-matching of engine with turbocharger and their applications. 2011 *International Conference on Electric Information and Control Engineering* 5, 1917–1920.

Mahmoudi, A. R., I. Khazaee and M. Ghazikhani (2017). Simulating the effects of turbocharging on the emission levels of a gasoline engine. *Alexandria Engineering Journal* 56(4), 737–748.

Mansouri, H. and F. Ommi. (2019). Performance Prediction of Aircraft Gasoline Turbocharged Engine at High-Altitudes. *Applied Thermal Engineering* 156 , 587–96.

Mizythras, P., E. Boulougouris and G. Theotokatos (2019). A Methodology for Single Turbocharger − Marine Engine Matching A Methodology for Single Turbocharger − Marine Engine Matching. In *Proceedings of the 2nd International Conference on Modelling and Optimization of Ship Energy Systems* (MOSES2019). Glasgow, Scotland, UK.

Moslemzadeh, M., A. Hajilouy and A. A. Mozafari (2014). Theoretical and Experimental Study of Turbocharging the Wankel Engine. Proceedings of the 8th International Conference on Internal Combustion Engines, Tehran, Iran. (in Persian)

Motahari, S. and I. Chitsaz (2019). Effects of Altitude and Temperature on the Performance and Efficiency of Turbocharged Direct Injection Gasoline Engine. *Journal of Applied Fluid Mechanics* 12 (6), 1825–36.

Okhuahesogie, O. F., J. Stewart, F. J. G. Heyes and P. E. R. Roach (2012). *Design optimization of two-stage turbocharger compressor impeller*. KTP Associates Conference, Brighton, UK.

Qiu, X., C. F. Fredriksson, N. C. Baines and M. Backlund (2013). *Designing Turbochargers With an Integrated Design System. Volume 5A: Industrial and Cogeneration; Manufacturing Materials and Metallurgy; Marine; Microturbines, Turbochargers, and Small Turbomachines*, 5 A, San Antonio, Texas, USA.

Roueini, A., M. Mirzabozorg and S. Kheradmand (2020). Developing a Mathematical Modelling Code for Keeping the Power of Multi Turbocharged Engines at Flight Altitudes." *Journal of Aerospace Technology and Management* 12 (April).

Sajedin, A. (2010). *Matching a Suitable Turbocharger with Natural Aspirated CNG Engine (EF7)*. Master thesis, K.N. Toosi University of Technology, Tehran, Iran. (in Persian)

Sanaye, S., S. Sedghi Ghadikolaee, M. M. Ghasemi and G. Rahimi (2015). A new approach for optimum selection of a turbocharger using a genetic algorithm. Proceedings of the Institution of Mechanical Engineers, Part D: *Journal of Automobile Engineering* 229(8), 1016–1033.

Shaabani Jafroudi, N., A. Hajilouy and A. Ehsandar (2010). Experimental Analysis of Modifications of a Natural Aspirated CNG Engine for Turbocharger Supplement. *Proceedings of the 18th International Conference on Mechanical Engineering*, Sharif University of Technology, Tehran, Iran. (in Persian)

Wiesbaden, S. F. (2018). Single-stage turbocharging has great potential. *MTZ Industrial* 8(2), 20–23.

Yang, M., C. Hu, Y. Bai, K. Deng, Y. Gu, Y. Qian and B. Liu (2019). Matching Method of Electric Turbo Compound for Two-Stroke Low-Speed Marine Diesel Engine. *Applied Thermal Engineering* 158 (July), 113752.

Yang, M., Y. Gu, K. Deng, Z. Yang and Y. Zhang (2018). Analysis on Altitude Adaptability of Turbocharging Systems for a Heavy-Duty Diesel Engine. *Applied Thermal Engineering* 128 (January), 1196–1207.

Zhang, Y., T. Chen, W. Zhuge, S. Zhang and J. Xu (2010). An integrated turbocharger design approach to improve engine performance. *Science in China Series E: Technological Sciences* 53(1), 69–74.